

AMELIORATION OF POOL BOILING THERMAL PERFORMANCE UTILIZING GNP-TIO₂ HYBRID NANOFLUID

*Yindong Song**, *Dongshu Yang*, *Linfeng Xiang*, *Zhiyun Zhang*

Jiangsu University of Science and Technology, Energy and Power Department, Zhenjiang, China

*Corresponding author; E-mail: songyindong@163.com

Hydrophobic graphene nanosheets were successfully modified with titanium dioxide to create a pure and stable nanoparticle. The resulting material exhibited improved heat transfer efficiency when used as nanofluid in pool boiling. We prepared graphene nanofluid, titanium dioxide nanofluid, and graphene-titanium dioxide hybrid nanofluid with varying concentrations to investigate their heat transfer characteristics. The heat transfer coefficient of graphene-titanium dioxide hybrid nanofluid is higher than that of water at the same heat flow density, especially in the low heat flow density region (below $q=4 \times 10^5 \text{ W/m}^2$). Additionally, by employing a high-speed camera, we observed that the hybrid nanofluid displayed shorter bubble generation periods and smaller bubble separation diameters. These findings highlight the exceptional heat transfer performance of the covalently modified and hybridized nanofluid. Overall, our comprehensive testing program confirms the enhanced heat transfer capabilities of this modified nanofluid, positioning it as a promising choice for various heat transfer applications.

Keywords: *Pool boiling; Heat transfer coefficient; Nanofluid; Bubble generation characteristics*

1. Introduction

Pool boiling is a critical heat transfer process in various fields such as power engineering [1], desalination [2,3], electronic equipment cooling [4], and heating systems [5]. Traditional heat transfer media like water, oil, and glycol have limited heat transfer performance due to their low thermal conductivity. To address the limitation of traditional media, extensive research has been conducted to optimize heat transfer processes [6].

In the late 18th century, Maxwell [7] proposed the addition of solid particles to liquids to enhance thermal conductivity. Recent advancements in material science have allowed the addition of nanoparticles in the nanometer range, leading to a groundbreaking achievement by Choi [8]. They successfully stabilized the suspension of nanoparticles in a base solution, introducing the concept of "nanofluid". nanofluid have superior thermal conductivity compared to traditional heat transfer media, making them a promising and innovative transport medium[9].

Hybrid nanofluid, created by combining two distinct nanomaterials, have altered thermal conductivity and stability, surpassing single-phase nanofluid [10]. Scholars have paid more attention to high thermal conductivity materials [34,35]. Yang and Liu [11] investigated the behavior of silica nanofluid under different atmospheric pressure conditions, while Park and Bang [12] conducted studies on graphene oxide, which demonstrated that nanofluid offer significant advantages in heat transfer. Same as titanium dioxide [13], zinc oxide [14, 15], copper oxide [16, 17], and silicon dioxide [18].

However, there is also evidence in the literature suggesting that nanoparticles have a negative impact on the boiling characteristics of the fluid. Nanoparticles reduce heat transfer by 40% at 4% volume concentration [19]. Similar findings were reported in studies by Das *et al* [20] and Milanova *et al* [21], which investigated three different types of nanofluid (aluminum trioxide, silica, and cerium dioxide (CeO₂)). Nanoparticle accumulation in Park *et al* [22] affected surface wettability and bubble behavior. These studies highlight the detrimental effect of nanoparticles on heat transfer efficiency in boiling systems. At lower volume concentrations, the nanoparticles were observed to have a positive effect on boiling.

Various studies have yielded inconclusive results on the impact of nanoparticles on boiling properties. Narayan [23] showed that the surface interaction parameter influences boiling performance, it can bring up to 70% enhancement. Chopkar *et al* [24] found that zirconia nanofluid enhances heat transfer but diminishes with increasing concentration. Sarafraz and Hormozi [25, 26] observed a higher CHF for low nanofluid concentration compared to pure water, decreasing with increasing concentration. Bolukbasi and Ciloglu [27] reported no significant effect on the heat transfer coefficient for silica nanofluid under specific conditions.

The impact of nanofluid on pool boiling characteristics is complex and influenced by factors such as nanoparticle shape, size, heating surface, volume concentration, and experimental conditions. The existing studies have focused on performance-oriented perspectives, but the lack of qualitative comparisons hinders insights from classical disciplines like fluid dynamics. Previous studies have shown that nanoparticles can enhance heat transfer by improving the thermal conductivity of fluids, but few have analysed it from the perspective of bubble dynamics.

The distinctive structure and surface attributes of graphene (GNP) facilitate the effective dispersion and stabilization of hybridized nanoparticles within nanofluid [28]. GNP and its complexes have attracted the attention of many researchers [30-33]. While titanium dioxide (TiO₂) nanofluid have been shown to have high pool boiling heat transfer efficiency [13]. The aforementioned advantages render GNP-TiO₂ nanofluid a promising avenue for the advancement of heat transfer technology, with the potential to enhance efficiency, curtail energy consumption, and facilitate sustainable development. The objective of this study is to examine the thermophysical and rheological properties of GNP-TiO₂ dioxide nanofluid, analyses their heat transfer characteristics, and gain a deeper understanding of the boiling heat transfer behavior.

2. Experimental methodology

2.1. Materials and Manufacturing

In this study, GNP was employed as the primary material, and hybridised nanoparticles were prepared by modifying functionalised GNP with TiO₂. The preparation process of GNP-TiO₂ hybrid nanoparticles involved addressing the issue of poor dispersion by introducing oxygen-containing functional groups through acid treatment (as shown in Fig. 1). Nanofluid were prepared using a two-step method with concentrations ranging from 0.001% to 0.005%.

The stability of the nanofluid was assessed by macroscopic observation, with no significant precipitation at the bottom of the reagent bottles after 36 h. The GNP-TiO₂ hybrid nanofluid showed higher dispersion stability due to the presence of oxygen-containing functional groups introduced during the functionalisation process.

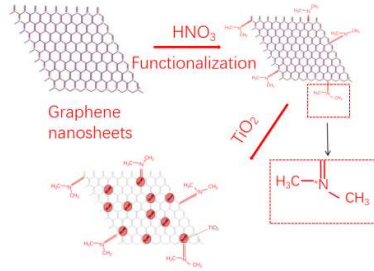


Figure 1. Schematic diagram of hybrid GNP preparation

2.2. Material phase and structure analysis

The crystalline purity of the GNP-TiO₂ hybrid nanoparticle was meticulously evaluated through X-ray diffraction (XRD) analysis. Concurrently, the identification of functional groups inherent to the hybrid material was ascertained via Fourier-transform infrared spectroscopy (FTIR). The synthesis of these analytical findings facilitated a comprehensive assessment of the interfacial adhesion strength and the degree of contamination between functionalized graphene and titanium dioxide nanoparticles. This integrative characterization approach underpins the determination of the hybrid material's viability for intended applications.

2.2.1. X-ray test

As shown in Fig.2, the X-ray Diffraction (XRD) pattern of GNP nanoparticles shows only one broad peak at about $2\theta=24.44^\circ$ indicating high purity. GNP-TiO₂ hybrid nanoparticles exhibits a similar pattern but with reduced intensity due to the tight binding between the two types of nanoparticles. TiO₂ nanoparticles exhibits prominent peaks at $2\theta=25.04^\circ$, $2\theta=37.97^\circ$, $2\theta=47.88^\circ$, and $2\theta=54.35^\circ$, corresponding to the crystalline indices (101), (004), (200), and (105), respectively, indicating a highly crystalline anatase phase structure.

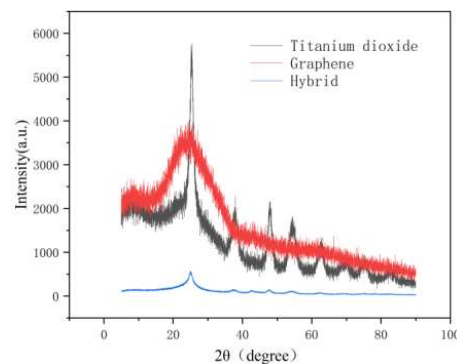


Figure 2. XRD profile of nanoparticles

2.2.2. FTIR test

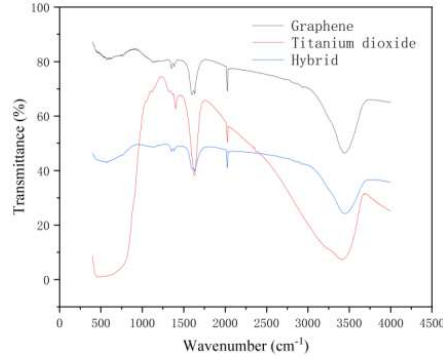


Figure 3. FTIR spectra of nanoparticles

As shown in Fig.3, TiO₂ nanoparticles exhibits absorption peaks at 1619.75cm⁻¹ (-OH vibration), 3430.73cm⁻¹ (water of crystallization), and 500.03cm⁻¹ (crystal structure). GNP nanoparticles shows absorption peaks at 587.96cm⁻¹ (C-O single bond), 1355.73cm⁻¹ (C=C bond in benzene-like ring), 1605.23cm⁻¹ (C=O bond in carboxyl group), and 3456.42cm⁻¹ (-OH bond). The spectra of GNP-TiO₂ shows hybrid nanoparticles indicated chemical bonds at characteristic peaks. These results confirm the successful doping of TiO₂ into the carbon skeleton and the functionalization of GNP through covalent reactions validated by FTIR spectroscopy.

2.3. Pool boiling experiment

2.3.1. Experimental setup

This study is the same as the previous experimental setup of Xiang L *et al* [30,36] (as shown in Fig. 4).

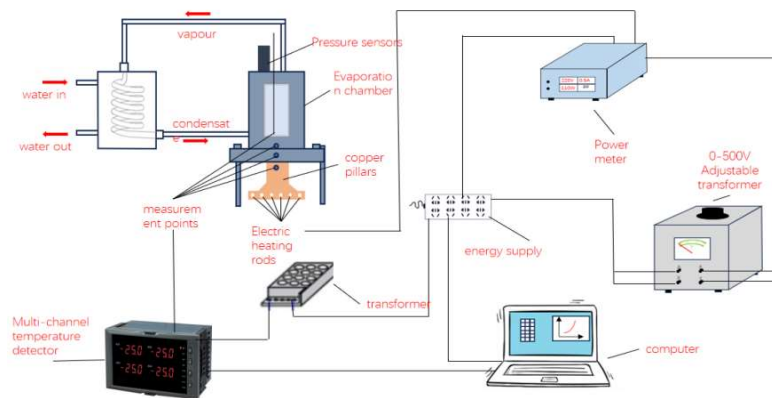


Figure 4. Experimental setup for pool boiling

2.3.2. Data uncertainty analysis

To ascertain the heat flow density of the heated fluid, it is essential to determine both the temperature of the heated surface (T_w) and the saturation temperature of the work fluid (T_s). However, the direct arrangement of thermocouple to read the temperatures produces considerable errors due to the presence of numerous nucleation sites on the heated surface and the significant fluctuations in the gas-liquid phase during the boiling process. In this study, extrapolation was employed to determine the boiling surface temperature.

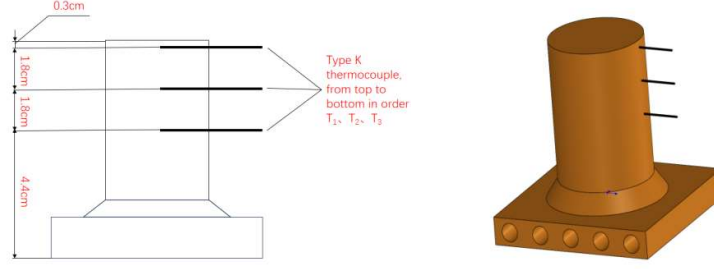


Figure.5 Diagram of Thermocouple Location

From the values of $T_1 \sim T_3$ (as shown in Fig.5), the heat flow density and wall temperature at the heated surface can be calculated. The experimental data uncertainty analysis have been clarified in previous articles [30].

The calculation formula is provided below:

$$q = \frac{1}{3} \lambda \left(\frac{T_2 - T_1}{\xi_1} + \frac{T_3 - T_2}{\xi_2} + \frac{T_3 - T_1}{\xi_1 + \xi_2} \right) \quad (1)$$

$$T_w = T_1 - \frac{q \cdot \xi_0}{\lambda} \quad (2)$$

Where, q represents the heat flow density, W/m^2 ; T_1, T_2, T_3 , represents three temperature measurement points of the thermocouple number, K.; respectively, ξ_1, ξ_2 represents the distance between T_2 and T_1, T_3 , m; λ represents the heating of the copper column of thermal conductivity, $W/m \cdot K$; T_w represents the heating of the copper column of the temperature of the surface of the heat transfer, K.

$$\Delta T = T_w - T_s \quad (3)$$

where T_s represents the saturation temperature of the work mass, K.

$$h = \frac{q}{\Delta T} = \frac{q}{T_w - T_s} \quad (4)$$

2.3.3. Setup reliability verification

The boiling curves of deionised (DI) water on a smooth copper surface were compared with the Rohsenow's correlation curve [29]. The experimental correlation curve proposed by Rohsenow can be expressed as:

$$\frac{c_{pl} \Delta T}{r} = C_{wl} \left[\frac{q}{\eta_l r \sqrt{g(\rho_l - \rho_v)}} \right]^{0.33} Pr_l^s \quad (5)$$

Where C_{pl} represents the specific heat capacity of saturated liquid at constant pressure, $J/(kg \cdot K)$; r represents the latent heat of vaporisation of the heat transfer medium, J/kg ; C_{wl} represents empirical constant that depends on the heating surface-liquid combination; η_l represents the kinetic viscosity of the saturated liquid, $Pa \cdot s$; σ represents the surface tension at the interface of liquid-vapour, N/m ; ρ_l and ρ_v represent the densities of saturated liquid and saturated vapour, kg/m^3 ; Pr_l^s represents the Prandtl number of the saturated liquid; and s represents the empirical exponent, with $s=1$ for water.

From the results of the validation experiments, it can be seen in Fig. 6 that the boiling curve of DI water on a smooth plane in the experimental system has a very similarity with the Rohsenow correlation curve, and the two curves do not differ by more than 5% in the range of ΔT between 10~18 K.

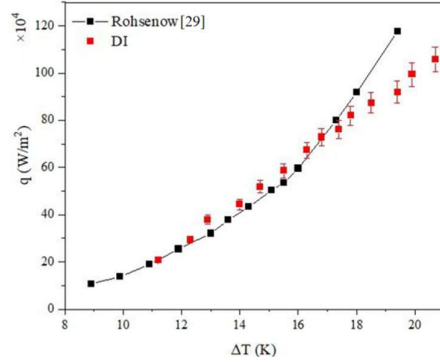


Figure 6. Comparison chart between experimental results and Rohsenow's correlation [29] equation

3.Results and discussion

3.1. Influence of different mass fractions

As shown in Fig.7, the Critical heat flux density (CHF) of GNP nanofluid with different mass fractions were $1.138 \times 10^6 \text{W/m}^2$, $1.273 \times 10^6 \text{W/m}^2$, $1.312 \times 10^6 \text{W/m}^2$, $1.210 \times 10^6 \text{W/m}^2$, and $1.430 \times 10^6 \text{W/m}^2$, with an enhancement of 7.6%, 20.4%, 24.1%, 14.5%, and 36.2% respectively compared to DI water. The heat flow density of GNP nanofluid was approximately linearly related to the ΔT .

The highest HTC of GNP nanofluid with different mass fractions were $5.23 \times 10^4 \text{W/m}^2 \times \text{K}$, $5.4 \times 10^6 \text{W/m}^2 \times \text{K}$, $5.47 \times 10^6 \text{W/m}^2 \times \text{K}$, $6.10 \times 10^6 \text{W/m}^2 \times \text{K}$, and $6.02 \times 10^6 \text{W/m}^2 \times \text{K}$, with an enhancement of 2.5%, 5.7%, 7.1%, 19.3%, and 17.8 % ,respectively compared to DI water.

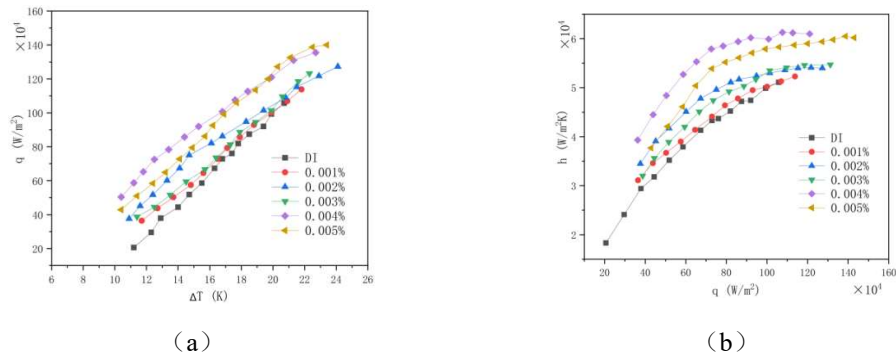


Figure 7. (a) boiling curves (b) heat transfer coefficient curves of GNP nanofluid

As shown in Fig. 8, the ΔT of TiO_2 nanofluid is lower than that of DI water at the same heat flux density, resulting in a left shift of the boiling curve, which suggests that TiO_2 nanofluid requires a smaller ΔT to initiate nucleation boiling. The Onset of Nucleate Boiling (ONB) of the TiO_2 nanofluid slightly fluctuates with concentration, and the ONB of TiO_2 nanofluid with different mass fractions is 9K, 8K, 8.9K, 8.6K, and 9.1K, which is lower than that of DI water by 2.2K, 3.2K, 2.3K, 2.6K, and 2.1K respectively.

The CHF of TiO_2 nanofluid with different mass fractions are $1.247 \times 10^6 \text{W/m}^2$, $1.318 \times 10^6 \text{W/m}^2$, $1.319 \times 10^6 \text{W/m}^2$, $1.313 \times 10^6 \text{W/m}^2$, and $1.370 \times 10^6 \text{W/m}^2$. Showing an enhancement of 17.9%, 24.7%, 24.8%, 24.2%, and 36.2% ,respectively compared to DI water.

The highest HTC of TiO_2 nanofluid with different mass fractions are $5.47 \times 10^4 \text{W/m}^2 \times \text{K}$,

$5.81 \times 10^4 \text{ W/m}^2 \times \text{K}$, $5.85 \times 10^4 \text{ W/m}^2 \times \text{K}$, $5.37 \times 10^4 \text{ W/m}^2 \times \text{K}$, and $5.44 \times 10^4 \text{ W/m}^2 \times \text{K}$, with an enhancement of 7%, 13.6%, 14.5%, 5.1%, and 6.4 %, respectively compared to DI water.

The heat transfer coefficient curves of the TiO_2 nanofluid indicated a diminishing growth with increasing heat flow density, and a decline at higher heat flow density. This suggests that although high heat flow density leads to increased surface ΔT , which makes bubble formation and detachment more frequent, but the process of bubble attachment and detachment triggers bubble aggregation phenomenon, which reduces the heat transfer effect. Besides nanoparticles may lead to deposition or clogging phenomenon under high heat flow density, which further reduces the heat transfer efficiency.

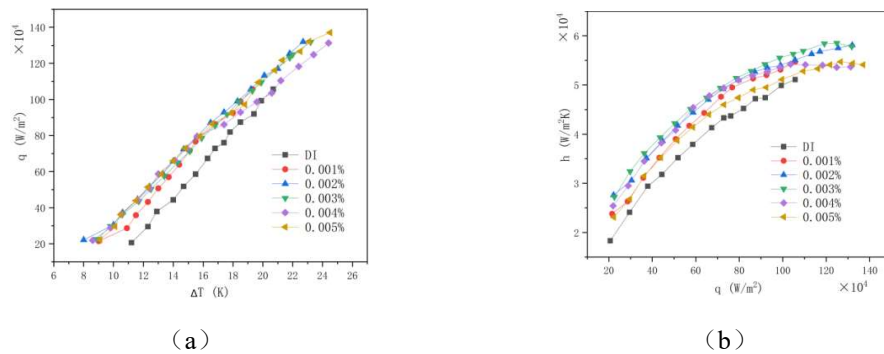


Figure 8. (a) boiling curves and (b) heat transfer coefficient curves of TiO_2 nanofluid

As shown in Fig.9, the CHF of GNP- TiO_2 nanofluid with different mass fractions were $1.109 \times 10^6 \text{ W/m}^2$, $1.153 \times 10^6 \text{ W/m}^2$, $1.223 \times 10^6 \text{ W/m}^2$, $1.282 \times 10^6 \text{ W/m}^2$, and $1.295 \times 10^6 \text{ W/m}^2$. Showing 4.9%, 9.8%, 15.7%, 21.3% and 22.5%, respectively compared to DI water.

The HTC of GNP- TiO_2 nanofluid is higher than that of DI water at the same heat flow density, especially in the low heat flow density region(below $q=4 \times 10^5 \text{ W/m}^2$). This suggests that GNP- TiO_2 hybrid nanofluid are excellent for industrial applications in the low heat flow density region, especially in the boiling initiation stage.

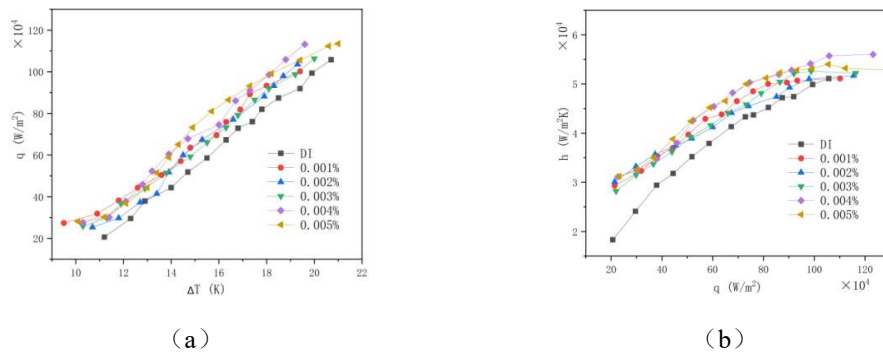
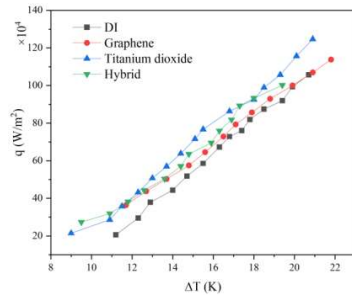


Figure 9. (a) boiling curves and (b) heat transfer coefficient curves of hybrid nanofluid

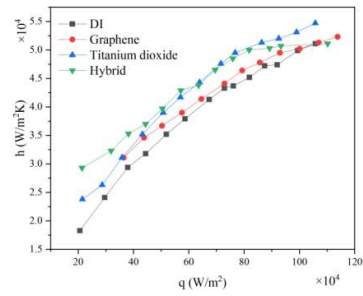
3.2. Influence of nanofluid type

As shown in Fig.10, at lower mass concentrations, TiO_2 nanofluid exhibit slightly better heat transfer performance due to their higher thermal conductivity, enhancing the overall boiling heat transfer capability. However, at higher mass concentrations, GNP nanofluid consistently outperform TiO_2 nanofluid and hybrid nanofluid. GNP nanofluid, especially at a mass concentration of 0.004%, demonstrate a 13.5% increase in maximum heat transfer coefficient compared to TiO_2 nanofluid and an

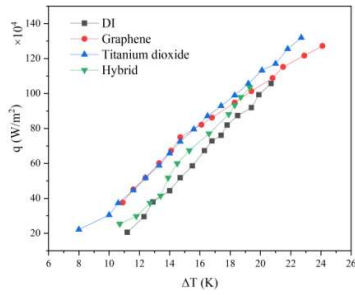
8.9% increase compared to hybrid nanofluid at the same concentration.



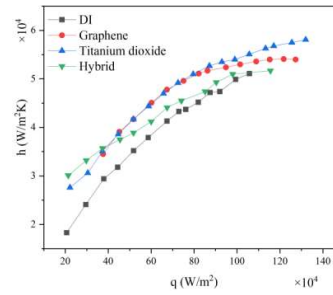
(a) Boiling curve of 0.001 wt%



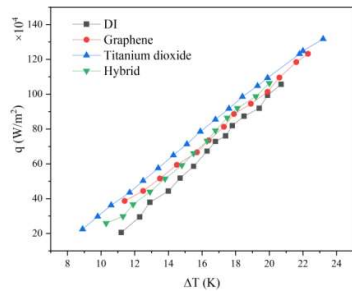
(b) HTC curve of 0.001 wt%



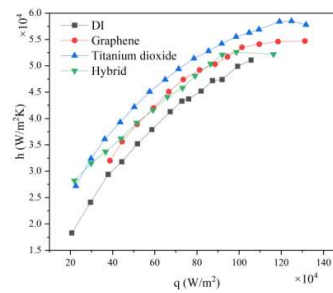
(c) Boiling curve of 0.002 wt%



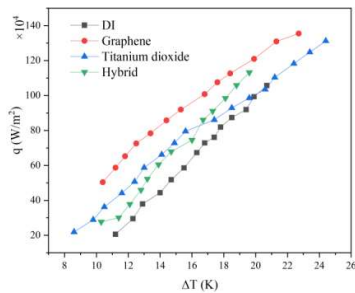
(d) HTC curve of 0.002 wt%



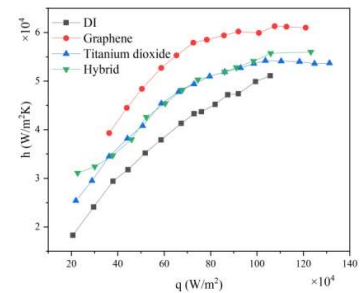
(e) Boiling curve of 0.003 wt%



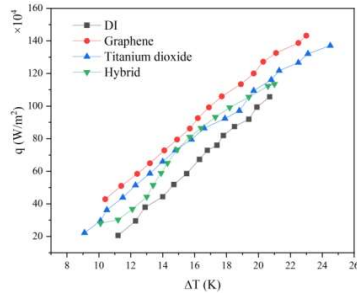
(f) HTC curve of 0.003 wt%



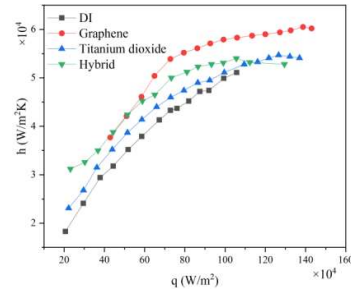
(g) Boiling curve of 0.004 wt%



(h) HTC curve of 0.004 wt%



(i) Boiling curve of 0.005 wt%



(j) HTC curve of 0.005 wt%

Figure 10. Boiling curves and HTC curves of nanofluid at the same mass concentration

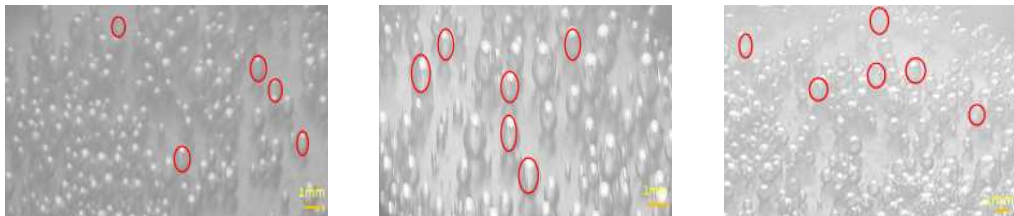
At $q=2 \times 10^5 \text{ W/m}^2$, the GNP-TiO₂ nanofluid with a mass concentration of 0.0003% has the highest HTC of $2.71 \text{ W/m}^2\text{K}$, which is a 42.4% enhancement with respect to water. The HTC of GNP-TiO₂ nanofluid with 0.0005% mass concentration has the highest HTC of $3.75 \text{ W/m}^2\text{K}$ at $q=4 \times 10^5 \text{ W/m}^2$, which is 30.3% higher than that of DI water. Therefore, GNP-TiO₂ can enhance heat transfer more effectively in the low heat flow density region, and the advantageous interval of this nanofluid is $2 \times 10^5 \sim 4 \times 10^5 \text{ W/m}^2$. In this range of heat flux density, the formation of vaporized cores is the main influencing factor of nanoparticles on cell boiling, which indicates that GNP-TiO₂ hybrid nanofluid can provide a better vaporization core in the initial stage of boiling.

3.3. Bubble generation characteristics

Both three type nanofluid demonstrate effective bubble cluster separation, reducing the bubble growth cycle and exposing the heated surface at a heat flow density of $q = 8 \times 10^5 \text{ W/m}^2$. This suggests that both nanoparticles enhance the affinity of the heated surface for water molecules, the small cross-sectional area at the bottom of the bubbles on the hydrophilic surface that favours lateral replenishment of the liquid near the heated surface, which can improve the fluid supply mechanism.

In order to investigate the effect of concentration on bubble detachment, the present study compares the bubble departure diameters at different nanofluid concentrations (wt% = 0.001, 0.003, 0.005, Fig. 11). At $q = 8 \times 10^5 \text{ W/m}^2$, the bubble detachment diameter increased with increasing heat flow density and decreasing nanofluid concentration. The formation, growth and detachment of individual bubbles follow a regular cycle during the heating process. The smaller the detachment diameter, the shorter the evolutionary cycle and the stronger the microfluidic interference. The smaller bubble departure diameter and higher detachment frequency of GNP-TiO₂ hybrid nanofluids compared to the other two nanofluids are attributed to the introduction of some oxygen-containing functional groups into the hybrid nanoparticles during the functionalisation process.

Higher concentration of nanofluid reduces the surface nucleation barrier, promoting the formation of nucleation sites through smaller cavities. However the tight build-up of bubbles under high heat flow density prevents the liquid from flowing back towards the surface, this leads to a reduction in the HTC.



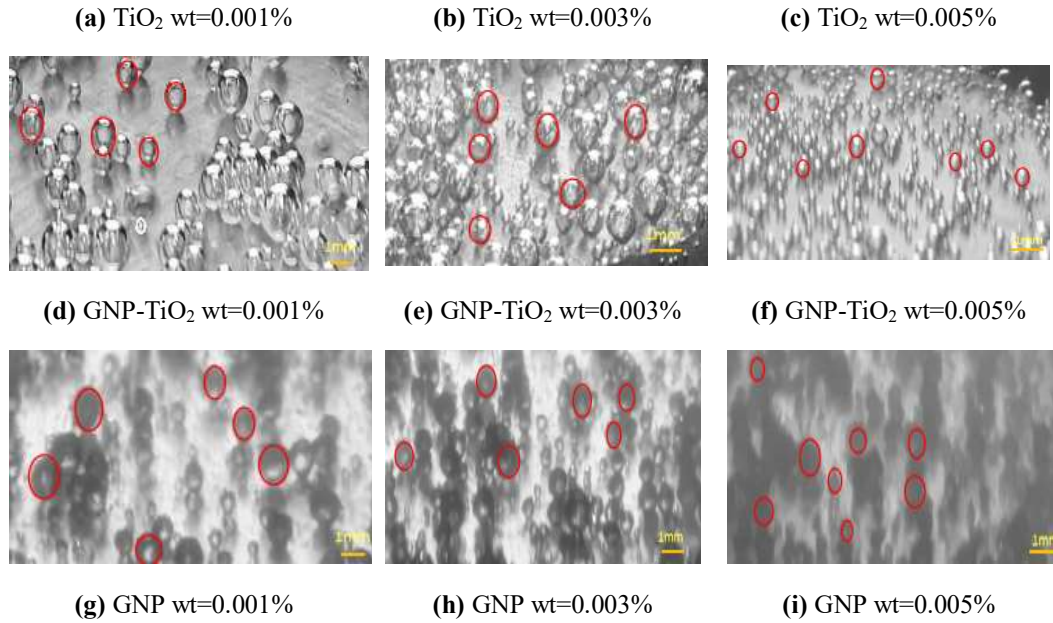


Figure 11. The bubbles on the heating surface of three nanofluid (red circles mark bubbles that are about to detach from the heating surface)

4. Conclusions

This study employed TiO_2 , GNP nanoparticles to prepare the novel GNP, TiO_2 and GNP- TiO_2 composite nanofluid. Subsequently, boiling heat transfer characteristics were compared among GNP, TiO_2 and GNP- TiO_2 composite nanofluid at different mass fractions (wt% = 0.001, 0.002, 0.003, 0.004, 0.005). Moreover, the heat transfer performance among different types of nanofluid at the same concentration was evaluated, leading to the following conclusions:

(1) Incorporating TiO_2 , and GNP- TiO_2 hybrid nanoparticles in deionized water shifted the advance and reduced the ΔT . wt%=0.002 of TiO_2 nanofluid ΔT at ONB is 3.2 K lower than that of DI water.

(2) At low heat flow density, GNP- TiO_2 hybrid nanofluid shows excellent boiling heat transfer performance. The heat transfer coefficient of GNP- TiO_2 hybrid nanofluid with wt%=0.002 is 17.9% higher than that of DI water at $q=4 \times 10^5 \text{ W/m}^2$.

(3) The GNP- TiO_2 hybrid nanoparticles exhibited smaller detachment diameter and higher detachment frequency during boiling onset, due to oxygen-containing functional groups. Smaller bubbles require less energy to form on the heated surface and can be generated and disengaged more quickly. This increases the frequency of bubble generation, which in turn increases the overall rate of heat transfer.

Nomenclature

CHF	Critical heat flux density
HTC	Heat transfer coefficient
ONB	Onset of Nucleate Boiling
h	Heat transfer coefficient

q	Heat flux density
T_w	Saturation temperature of the heated wall
T_s	Saturation temperature of the work mass
GNP	Graphene
TiO ₂	Titanium dioxide
DI	Deionized

Reference

- [1] MAFFEZZONI C. Boiler-Turbine Dynamics in Power Plant Control[J/OL]. IFAC Proceedings Volumes, 1996, 29(1): 6843-6854.
- [2] HUMPLIK T, LEE J, O'HERN S C, *et al.* Nanostructured materials for water desalination[J/OL]. Nanotechnology, 2011, 22(29): 292001.
- [3] MESSER M, ANDERSON K, ZHANG X, *et al.* Effect of surface roughness on mixed salt crystallization fouling in pool boiling[J/OL]. DESALINATION AND WATER TREATMENT, 2022, 274: 219-229.
- [4] POP E. Energy dissipation and transport in nanoscale devices[J/OL]. Nano Research, 2010, 3(3): 147-169.
- [5] AYAD F, BENELMIR R, SOUAYED A. CO₂ evaporators design for vehicle HVAC operation[J/OL]. Applied Thermal Engineering, 2012, 36: 330-344.
- [6] BAHIRAEI M, MAZAHERI N, RIZEHVANDI A. Application of a hybrid nanofluid containing graphene nanoplatelet–platinum composite powder in a triple-tube heat exchanger equipped with inserted ribs[J/OL]. Applied Thermal Engineering, 2019, 149: 588-601.
- [7] MAXWELL J. A Treatise on Electricity and Magnetism, I: 1[M]. 1892.
- [8] CHOI S U S, EASTMAN J A. Enhancing Thermal Conductivity of Fluids with Nanoparticles[J].
- [9] Xuan Y ; Theory and application of energy transfer in nanofluids[J](in Chinese). China Science:Technical Sciences, 2014(03 vo 44): 269-279.
- [10] SUNDAR L S, SHARMA K V, SINGH M K, *et al.* Hybrid nanofluid preparation, thermal properties, heat transfer and friction factor – A review[J/OL]. Renewable and Sustainable Energy Reviews, 2017, 68: 185-198.
- [11] YANG X, LIU Z hua. A Kind of nanofluid Consisting of Surface-Functionalized Nanoparticles[J/OL]. Nanoscale Research Letters, 2010, 5(8): 1324-1328.
- [12] PARK S D, BANG I C. Experimental study of a universal CHF enhancement mechanism in nanofluid using hydrodynamic instability[J/OL]. International Journal of Heat and Mass Transfer, 2014, 70: 844-850.
- [13] ALI H M, GENEROUS M M, AHMAD F, *et al.* Experimental investigation of nucleate pool boiling heat transfer enhancement of TiO₂-water based nanofluid[J/OL]. Applied Thermal Engineering, 2017, 113: 1146-1151.
- [14] KOLE M, DEY T K. Thermophysical and pool boiling characteristics of ZnO-ethylene glycol nanofluid[J/OL]. International Journal of Thermal Sciences, 2012, 62: 61-70.
- [15] KOLE M, DEY T K. Investigations on the pool boiling heat transfer and critical heat flux of ZnO-ethylene glycol nanofluid[J/OL]. Applied Thermal Engineering, 2012, 37: 112-119.
- [16] SHOGHL S N, BAHRAMI M. Experimental investigation on pool boiling heat transfer of ZnO, and CuO water-based nanofluid and effect of surfactant on heat transfer coefficient[J/OL].

- International Communications in Heat and Mass Transfer, 2013, 45: 122-129.
- [17] LIU Z H, XIONG J G, BAO R. Boiling heat transfer characteristics of nanofluid in a flat heat pipe evaporator with micro-grooved heating surface[J/OL]. International journal of Multiphase Flow, 2007, 33(12): 1284-1295.
- [18] NOROUZIPOUR A, ABDOLLAHI A, AFRAND M. Experimental study of the optimum size of silica nanoparticles on the pool boiling heat transfer coefficient of silicon oxide/deionized water nanofluid[J/OL]. Powder Technology, 2019, 345: 728-738.
- [19] BANG I C, HEUNG CHANG S. Boiling heat transfer performance and phenomena of Al₂O₃-water nano-fluids from a plain surface in a pool[J/OL]. International Journal of Heat and Mass Transfer, 2005, 48(12): 2407-2419.
- [20] DAS S K, PUTRAN, ROETZEL W. Pool boiling characteristics of nano-fluids[J/OL]. International Journal of Heat and Mass Transfer, 2003, 46(5): 851-862.
- [21] MILANOVA D, KUMAR R. Role of ions in pool boiling heat transfer of pure and silica nanofluid[J/OL]. Applied Physics Letters, 2005, 87(23).
- [22] PARK H, LEE S J, JUNG S Y. X-ray imaging analysis on behaviors of boiling bubbles in nanofluid[J/OL]. International Journal of Heat and Mass Transfer, 2019, 128: 443-449.
- [23] NARAYAN G P, ANOOP K B, DAS S K. Mechanism of enhancement/deterioration of boiling heat transfer using stable nanoparticle suspensions over vertical tubes[J/OL]. Journal of Applied Physics, 2007, 102(7).
- [24] CHOPKAR M, DAS A K, MANNA I, *et al.* Pool boiling heat transfer characteristics of ZrO₂-water nanofluid from a flat surface in a pool[J/OL]. Heat and Mass Transfer, 2008, 44(8): 999-1004.
- [25] SARAFAZ M M, HORMOZI F. Nucleate pool boiling heat transfer characteristics of dilute Al₂O₃-ethyleneglycol nanofluid[J/OL]. International Communications in Heat and Mass Transfer, 2014, 58: 96-104.
- [26] SARAFAZ M M, HORMOZI F. Pool boiling heat transfer to dilute copper oxide aqueous nanofluid[J/OL]. International Journal of Thermal Sciences, 2015, 90: 224-237.
- [27] BOLUKBASI A, CILOGLU D. Pool boiling heat transfer characteristics of vertical cylinder quenched by SiO₂-water nanofluid[J/OL]. International Journal of Thermal Science, 2011, 50(6): 1013-1021.
- [28] RASHEED A K, KHALID M, RASHMI W, *et al.* Graphene based nanofluid and nanolubricants - Review of recent developments[J/OL]. RENEWABLE & SUSTAINABLE ENERGY REVIEWS, 2016, 63: 346-362.
- [29] Rohsenow W M .A Method of Correlating Heat Transfer Data for Surface Boiling Liquids[J].trans asme, 1951.
- [30] XIANG L, SONG Y, YANG D, *et al.* Experiments and modeling of boiling heat transfer of GNP nanofluid with metallic elements[J/OL]. Experimental Heat Transfer, 2023: 1-18.
- [31] SONG Y, MA X, WANG Y, *et al.* Amelioration of boiling heat transfer by 3D deposition structure of graphene-silver hybrid nanoparticle[J/OL]. Energy Conversion and Management: X, 2021, 12: 100109.
- [32] MA X, SONG Y, WANG Y, *et al.* Amelioration of pool boiling thermal performance utilizing graphene-silver hybrid nanofluid[J/OL]. Powder Technology, 2022, 397: 117110.
- [33] MA X, SONG Y, WANG Y, *et al.* Experimental study of boiling heat transfer for a novel type of GNP-Fe₃O₄ hybrid nanofluid blended with different nanoparticles[J/OL]. Powder Technology,

2022, 396: 92-112.

- [34] S. Z. Heris, S. G. Etemad, and M. N. Esfahany, "Experimental investigation of metal oxide nanofluid convection heat transfer," *J. Math.*, vol. 1920, p. 181, 2005.
- [35] V. S. Korada, S. K. Vandrangi, S. Kamal, and A. A. Minea, "Experimental Studies on the Influence of Metal and Metal Oxide nanofluid Properties on Forced Convection Heat Transfer and Fluid Flow," *Adv. New Heat Transfer Fluids*, 2017.
- [36] XIANG L, SONG Y, YANG D, et al. Boiling mechanism of biphilic surfaces based on Helmholtz instability and Taylor instability[J/OL]. *International Journal of Multiphase Flow*, 2024: Volume 173.

- Paper submitted: 19 October 2024
- Paper revised: 6 March 2025
- Paper accepted: 7 March 2025